Progress in Reaction Kinetics and Mechanism. Vol. 36, pp. 63–72. 2011
doi: 10.3184/146867810X12925913885222 1468-6783 © 2011 Science Reviews 2000 Ltd

RESEARCH PAPER

A computational study of the kinetics and mechanism of the gas phase pyrolysis of allyl methyl amine

Mohammad Izadyar[a*], *Effat Esmaili*[b] *and Mohammad Harati*[c]

[a]*Department of Chemistry, Ferdowsi University of Mashhad, Mashhad, I.R. Iran*

[b]*Department of Chemistry, Ganobad University of Payam Noor, Khorasan-e-Razavi, Iran*

[c]*Department of Chemistry and Biochemistry, University of Windsor, Ontario, Canada N9B 3P4*

**E-mail: Izadyar@um.ac.ir*

ABSTRACT

A density functional theory (DFT) study has been carried out at the B3LYP/6–31G(d) level on the gas-phase retro-ene reaction of allyl methyl amine (AMN). The results were compared with single point calculations at a high level of the theory, using the G3MP2 method. Two mechanisms for this kind of reaction are possible, one involves a six-membered cyclic transition state (TS) and the other is a multistep, free radical mechanism. Both DFT and high level calculations show that propene and imine formation are in accordance with a concerted cyclic mechanism. Natural bond orbital analysis (NBO) and atoms-in-molecule (AIM) procedures show that the reaction achieves a synchronicity value of 90%. The calculated kinetic parameters for AMN pyrolysis agree with the available experimental results.

KEYWORDS: allyl methyl amine, pyrolysis, gas phase, concerted mechanism, DFT, retro-ene reaction, synchronicity

INTRODUCTION

Interest in the synthesis and theoretical studies of retro-ene reactions have increased considerably, because they are powerful tools for the synthesis of heterounsaturated compounds [1–4]. Our studies on the retro-ene reactions of organo-sulfur and unsaturated amines have shown that the interaction of S, O and N atoms on the H atom migration towards an unsaturated system can exert a strong chemical control [5–16]. Kinetic investigations and mechanisms of these

reactions have been the subject of some controversies in recent years [5 – 20]. However, it is not straightforward to be sure which mechanism operates under different conditions.

The most important mechanisms that are involved in the gas phase for retro-ene reactions include free radical chain and concerted processes. In previous studies, we have reported the thermal decomposition of some unsaturated organo-sulfur compounds from the kinetic and mechanistic approach. Based on our experimental and theoretical researches using different reactants, either a free radical mechanism or concerted one was proposed.

The gas phase pyrolysis of allyl methyl amine (AMN) has been studied by Martin *et al*. at 673 – 773 K [21]. The experimentally obtained rate equation corresponds to Eqn (1):

$$k(s^{-1}) = 10^{11.4} \exp(-181.6\,kJ\,mol^{-1}\,(RT)^{-1} \quad (1)$$

$$R = 8.314\,J\,mol^{-1}K^{-1}$$

They showed that there was no difference in rate in the presence nor absence of a free radical inhibitor and a concerted mechanism was proposed. This retro-ene reaction leads to the formation of propene and methanimine through six-centred TS (Scheme 1). Noting that the size of a molecule is a key parameter in utilising a computational method in calculations of energies and geometrical parameters, we have found that DFT methods are useful for the study of fairly large systems, and accordingly we have applied the B3LYP/6 – 31G(d) method [22,23] to investigate comprehensively the kinetics and mechanism of pyrolysis of AMN in the gas phase.

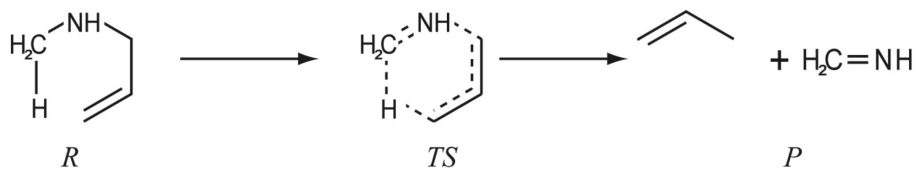

Scheme 1 (R = Reactant, TS = Transition State, P = Products)

This constitutes part of our research programme devoted to the kinetic and mechanistic study of retro-ene eliminations by theoretical procedures. In order to allow comparison between the theoretical and experimental results of Martin *et al*. [21], a set of single point calculations are provided.

Computational procedure

The structures corresponding to the reactant (R), transition state (TS) and products (P) for the given reaction were optimized using the GAUSSIAN 98 computational package [24] with the DFT method. Optimized geometries of the stationary points on the potential energy surfaces (PES) were obtained using Becke's three-parameter hybrid exchange functional with the correlation functional of Lee–Yang–Parr (B3LYP). In all of these calculations, we used 6–31G(d) as the main basis set. The corresponding TS structure was obtained using the synchronous transit-guided quasi-Newton (STQN) method as implemented by Schlegel *et al*. [25].

Vibrational frequencies for the points along the reaction paths were determined to provide an estimation of the zero point vibrational energies (ZPVE). There are also important in diagonalization of the Hessian matrix.

Activation parameters were calculated in the temperature range of the pyrolysis reaction (648 K). The activation energy, E_a, and the Arrhenius factor were computed using Eqns (2) and (3), respectively, as derived from transition state theory [26,27]:

$$E_a = \Delta H^{\neq}(T) + (RT) \tag{2}$$

$$A = ek_B T/h \exp(\Delta S^{\neq}(T)/R) \tag{3}$$

The natural bond orbital analysis, suggested by Reed *et al*. [28], was applied to determine the charges (q_i) at the stationary points through the pyrolysis reaction. The enthalpy (ΔH), entropy (ΔS) and Gibbs free energy (ΔG) of the reaction were evaluated from the B3LYP data under standard conditions.

In order to achieve a very precise image of the timing and extent of the bond breaking and bond formation processes at the stationary points of the reaction, it is necessary to evaluate and analyse the bond indices corresponding to the bond being made or broken. Thus it is convenient to define a relative variation of bond index at the TS (δB_i) for every bond (i) involved in a chemical reaction according to Moyano *et al*. [29] [Eqn (4)]:

$$\delta_{Bi} = \left(Bi^{TS} - Bi^{R}\right)/\left(Bi^{P} - Bi^{R}\right) \tag{4}$$

$$\delta_{Bav} = \sum_{i=1}^{n} \delta_{Bi}/n \tag{5}$$

where the superscripts R, TS and P refer to the reactants, transition state and products, respectively. Information from δ_{Bi} can be related to their average value (δ_{Bav}) according to Eqn (5).

It is important to note that definition of asynchronicity could be helpful in the clarification of the long-lasting dispute on the synchronous or asynchronous natures of concerted reactions that are allowed in the Woodward–Hoffmann sense, such as the Diels–Alder reaction, the 1,3-dipolar cycloadditions, the Claisen, the Cope [3,3]-sigmatropic rearrangements, and some of the retro-ene reactions. One can easily obtain information on the absolute asynchronicity (A_{syn}) of a chemical reaction, defined as in Eqn (6):

$$A_{syn} = 1 - (2n - 2)^{-1} \sum_{i=1}^{n} |\delta_{Bi} - \delta_{Bv}|/\delta_{Bav} \tag{6}$$

where n is the number of bonds directly involved in the reaction under consideration.

RESULTS AND DISCUSSION

Propene elimination from AMN can occur through the two possible mechanisms. The first may be initiated by the homolytic C4–N5 bond cleavage (for atom numbering see Figure 1), followed by a stepwise mechanism (Scheme 2).

The second possibility is the interamolecular transfer of the H1-atom to an unsaturated centre via a six-membered cyclic TS, yielding propene and methanimine. This can proceed through the H1—C2 bond formation and C4—N5 bond cleavage.

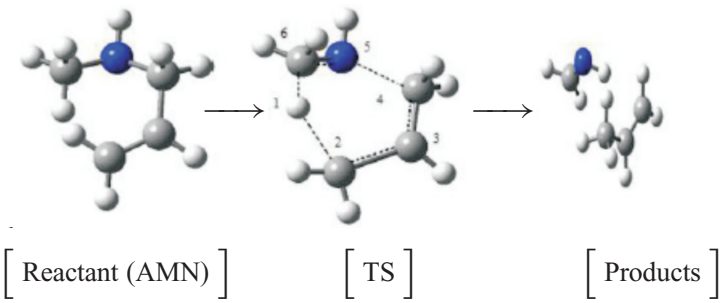

Figure 1 Atom numbering for AMN pyrolysis.

The C4—N5 bond breaking is the rate-determining step in the former mechanism. The bond dissociation energy of C4—N5 would be the main component of the activation barrier of this process from the energy point of view (Scheme 2).

$$CH_3NHC_3H_5 \longrightarrow CH_3NH^{\cdot} + {}^{\cdot}C_3H_5$$

$$CH_3NHC_3H_5 + {}^{\cdot}C_3H_5 \longrightarrow {}^{\cdot}CH_2NHC_3H_5 + C_3H_6$$

$${}^{\cdot}CH_2NHC_3H_5 \longrightarrow CH_2{=}NH + {}^{\cdot}C_3H_5$$

$${}^{\cdot}C_3H_{5+}\,{}^{\cdot}C_3H_5 \longrightarrow C_6H_6$$

Scheme 2 Radical mechanism

A high level of G3MP2 theory was applied to calculate the energies of the probable radicals (from Scheme 2) after full geometric optimization at the B3LYP level of the theory.

The results are shown in Table 1. It is obvious that the calculated activation energy is 305 kJ mol^{-1} for AMN pyrolysis. The calculated activation energy is much greater than the experimental value (181.6 kJ mol^{-1}). As attempts to locate a diradical minimum on the potential energy surface (PES) were unsuccessful, we focused on the concerted mechanism (Scheme 1).

During the retro-ene reaction, the H1—C2, C3—C4 and N5—C6 bond lengths are decreased, while the H1—C6, C4—N5 and C2—C3 bond lengths are increased. Geometric parameters for the reactant and the TS are reported in Table 2. Comparison between the H1—C2 and C4—N5 bond lengths in the TS with the same ones in the reactant indicates that H1—C2 bond formation occurs faster than C4—N5 bond scission. Accordingly, the new bond formation occurs with a slightly asynchronous nature in the concerted mechanism.

Table 1 Calculated total energies in kJ mol^{-1} for some probable radicals at the G3MP2/6–31G(d) level ZPVE are included

CH_3NH	C_3H_5	CH_3	C_3H_5NH	$CH_2NHC_3H_5$
−95.02	−116.87	−39.75	−172.28	−212.15

Table 2 Main geometric parameters for AMN (R) and the TS in the gas phase, using the B3LYP/6 – 3IG(d) method (distances in Angstroms (Å) and dihedrals in degrees (°)

Parameter	R	TS
H1 – C2	2.89	1.38
C2 – C3	1.33	1.41
C3 – C4	1.51	1.39
C4 – N5	1.45	2.01
H1 – C2 – C3	80.82	98.15
C2 – C3 – C4	126.45	118.24
C3 – C4 – N5	118.53	104.71
C4 – N5 – C6	114.90	112.12
H1 – C2 – C3 – C4	80.82	98.15
C2 – C3 – C4 – N5	126.45	118.24

The summary of the intrinsic reaction coordinate analysis (IRC) for the potential energy surface (PES) is shown as Figure 2. The PES demonstrates the energy as a function of the reaction coordinates, H1—C2 bond length, and represents the minimum energy path which connects the reactant to the products passing through the saddle point.

The evolution of net charges on the atoms along the reaction path is summarized in Table 3. As can be readily seen, these charges describe the TS as zwitterionic, with net charges of opposite sign placed at H1, C2 and C4, N5. The positive character of the H1 at the TS allows it to be attracted by the negative character of C2. On the other hand, the positive character of N5 and negative

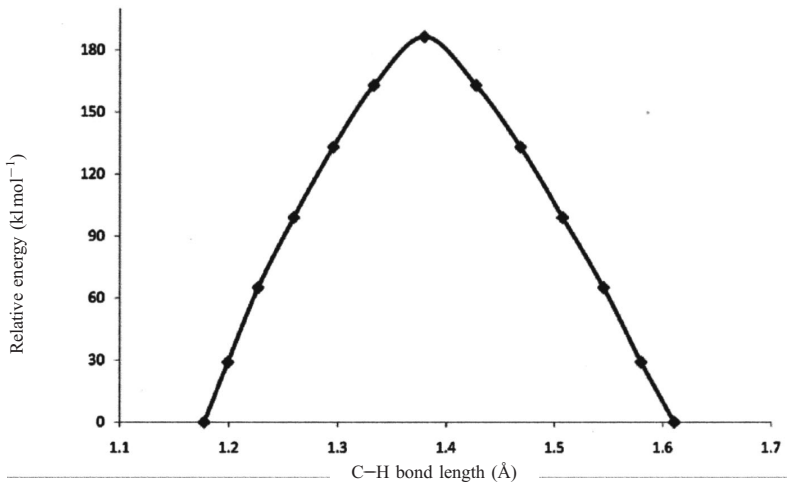

Figure 2 Schematic energy profile for AMN pyrolysis.

Table 3 NBO charges at the B3LYP/6−31G(d) level

	q_1	q_2	q_3	q_4	q_5	q_6
R	0.19	−0.45	−0.23	−0.29	−0.69	−0.47
TS	0.22	−0.57	−0.26	−0.36	−0.64	−0.36

character of C4 demonstrate that the H1—C2 bond formation does not happen at the same rate of the C4—N5 bond cleavage, so the reaction supports some degree of asynchronocity.

Imaginary vibrational frequencies for the TS were also obtained from the Hessian matrix. The high magnitude of this frequency (1,904 cm^{-1}) shows that these points are associated with the light atom movement of H1 in the TS, according to relationship between the fundamental vibrational frequency (ν) and the reduced mass (μ).

Dipole moment changes through the retro-ene reaction justify the greater polarity of the TS as compared to the reactant at four levels of theory. Table 4 shows that the reactant is more symmetric than the TS, confirmed the cyclic structure for the TS.

The calculated kinetic and activation parameters for the reaction at 648 K are listed in Table 5 using Eqns (2) and (3). We can conclude that the B3LYP results are the best ones from the activation energy point of view according to previous studies [5–16]. On the other hand, single point energy calculations at the G3MP2 and MP2 levels of the theory produced nearly as good results, $\Delta E^{\neq} = 207.55$ kJ mol^{-1} for the G3MP2 and 219.61 kJ mol^{-1} for the MP2, in contrast to the configuration interaction (CI) and HF data, $\Delta E^{\neq} = 242.35$ kJ mol^{-1} for the CI and 339.03 kJ mol^{-1} for the HF. These poor results can be due to the absence of free radicals during the reaction and the neglect of electron

Table 4 Calculated dipole moments using the 6−31G(d) basis set

Method	Reactant	TS
HF	0.81	1.78
MP2	0.96	1.76
QCISD(T)	0.97	1.76
G3MP2	0.83	1.69
B3LYP	0.70	1.54
	xx = −33.2	xx = −35.2
	yy = −31.6	yy = −31.4
	zz = −32.0	zz = −30.5

Table 5 Calculated kinetic and activation parameters for the pyrolysis of AMN at 626.65 K at the B3LYP level (E_a, $\Delta H^{\neq}$, $\Delta G^{\neq}$ in kJ mol^{-1} and $\Delta S^{\neq}$ in J mol^{-1} K^{-1})

E_a	$\Delta H^{\neq}$	log A	$\Delta G^{\neq}$	$-\Delta S^{\neq}$
186.36	181.15	12.8	190.12	14.31

Table 6 Evolution of relative bond indices and asynchronicity along the reaction coordinate for AMN pyrolysis according to the B3LYP method

	H1 – C2	C2 – C3	C3 – C4	C4 – N5	N5 – C6	C6 – H1
R	0	1.98	1.02	1.01	1.00	0.93
TS	0.45	1.37	1.47	0.48	1.40	0.45
P	0.98	0.93	1.90	0	2.03	0
%Ev	45.9	58.1	51.1	52.5	38.8	51.6
%Asyn			10.15			

correlation in energy calculations, respectively. The negative sign for the activation entropies show that retro-ene reaction proceeds through a concerted cyclic TS, as confirmed experimentally.

To analyse the extent of bond breaking and bond making through the course of reaction, the bond order concept has been applied and the Wiberg bond indices have been calculated using AIM analysis. The nature of the concerted mechanism has been monitored by means of the asynchronicity (A_{syn}) concept and the results are reported in Table 6. The results of bond index analysis of the reaction fully confirmed what was anticipated by inspection of the geometry of the TS. According to Table 6, approximately 58% of the initial C2—C3 bond and 53% of the initial C4—N5 bond have already vanished at the TS, whereas approximately 46% of the H1—C2 bond and only 39% of the N5—C6 bond have formed at this stage. In terms of bond index, this method predicts a transition state halfway between the reactant and the products ($\delta_{Bav} = 47\%$) and the overall process being described as a substantially synchronous mechanism ($A_{syn} = 10\%$).

Table 7 Computed activation parameters for allyl compounds

Reactant	E_a (kJ mol^{-1})	$-\Delta S^{\neq}$ (J mol^{-1} K^{-1})
$CH_3SC_3H_5$	154.56	19.90
$CH_3OC_3H_5$	167.51	24.10
$CH_3NHC_3H_5$	186.36	14.31

Table 8 Thermodynamic properties for the AMN reaction, using the B3LYP method

ΔH (kJ mol^{-1})	ΔS (J mol^{-1}K^{-1})	ΔG (kJ mol^{-1})
19.76	170.68	−31.15

Finally, according to all data, an important bond deficiency exists in the transition state, with bond cleavage processes being more advanced than the bond formation ones, and this translates into the important zwitterionic character reflected by the net atomic charges (q_i) on the atoms (Table 3).

The calculated activation energies and entropies at the B3LYP level for some allyl alkyl heteroatomic compounds in the gas phase are listed in Table 7. As can be seen, AMN has the lowest reactivity in comparison to allyl methyl ether and allyl methyl sulfide. Our interpretation of the lowest reactivity in the amine is that the hydrogen atom on the α-carbon of the alkyl group possesses a less acidic character.

Thermodynamic parameters for the reaction at the B3LYP level of the theory are reported in Table 8. The computed values show that the retro-ene reaction is endothermic, the global process is spontaneous, and the entropy increases during reaction, (*i.e.* $\Delta H > 0$, $\Delta G < 0$, $\Delta S > 0$).

ACKNOWLEDGEMENTS

The authors thank K. Golbaf, J. Momeni (Gonabad University of Payam-e-Noor) and N. Zamani (Education Organization of Khorasan-e-Razavi) for helpful discussions.

REFERENCES

[1] Brown, R.F.C. (1980) In: Wasserman, R.H. (ed.) *Pyrolytic methods in organic chemistry*, Academic Press, New York, 229.
[2] Hoffmann, H.M.R. (1969) *Angew. Chem.*, **81**, 597.
[3] Dubac, J. and Laporterie, A. (1987) *Chem. Rev.*, **87**, 319.
[4] Viola, A., Collins, J.J. and Fillip, N. (1981) *Tetrahedron*, **37**, 3765.
[5] Gholami, M.R. and Izadyar, M. (2002) *Proc. 6th Iranian Physical Chemistry Seminar*, Urmia University, Iran, 31.
[6] Gholami, M.R. and Izadyar, M. (2003) *J. Phys. Org. Chem.*, **16**, 153.
[7] Izadyar, M., Gholami, M.R. and Haghgu, M. (2004) *14th Iranian Chemistry and Chemical Engineering Conference*, 754.
[8] Gholami, M.R. and Izadyar, M. (2004) *J. Mol. Struct. (THEOCHEM)*, **672**, 61.

[9] Izadyar, M., Jahangir, A.H. and Gholami, M.R. (2004) *J. Chem. Res*., **11**, 585.
[10] Izadyar, M., Gholami, M.R. and Haghgu, M. (2004) *J. Mol. Struct. (THEOCHEM)*, **686**, 37.
[11] Gholami, M.R. and Izadyar, M. (2004) *Chem. Phys*., **301**, 45.
[12] Izadyar, M. and Gholami, M.R. (2006) *J. Molec. Struct. (THEOCHEM)*, **759**, 11.
[13] Izadyar, M. and Zamani, N. (2007) *The Book of Finite Elelments*, WSEAS Press, 159.
[14] Izadyar, M., Jahangir, A.H. and Gholami, M.R. (2004) *International Conference of Chemistry*, ICCMSE.
[15] Izadyar, M. and Esmaili, E. (2010) *13th Iranian Physical Chemistry Seminar*, Shiraz University of Technology, 359.
[16] Izadyar, M. and Harati, M. (2010) *93rd Canadian Chemistry Conference and Exhibition*, 242.
[17] Molera, M.J. and Lopez, J.A. (1958) *J. Am. Chem. Soc*., **54**, 127.
[18] Martin, G. and Ascanio, J. (1991) *J. Phys. Org. Chem*., **4**, 579.
[19] Quiros, J.A.L. and Molera, M.J. (1954) *J. Am. Chem. Soc*., **50**, 851.
[20] Rodriguez, L.J., Anez, R. and Ocando-Mavarez, E. (2001) *J. Mol. Struct. (THEOCHEM)*, **536**, 53.
[21] Martin, G., Ropero, M. and Avila, R. (1982) *Phosphorus Sulfur*, **13**, 213.
[22] Becke, A.D. (1993) *J. Chem. Phys*., **98**, 5648.
[23] Lee, C., Yang, W. and Parr, R.G. (1988) *Phys. Rev. B*., **371**, 785.
[24] Gaussian 98 (1998) Revision A.9 Gaussian Inc., Pittsburgh, PA.
[25] Schlegel, H.B., Peng, C., Ayala, P.Y. and Frisch, M.J. (1996) *J. Comput. Chem*., **17**, 49.
[26] Laidler, K.J. (1969) *Theories of chemical reaction rates*, McGraw-Hill, New York.
[27] Glasstone, S., Laidler, K.J. and Eyring, H. (1941) *The theory of rate processes*, McGraw-Hill, New York.
[28] Reed, A.E., Weinstock, R.B. and Weinhold, F. (1983) *J. Chem. Phys*., **78**, 4066.
[29] Moyano, A., Pricas, M.A. and Valenti, A. (1989) *J. Org. Chem*., **54**, 573.